Deacylation and Reacylation for a Series of Acyl Cysteine Proteases, Including Acyl Groups Derived from Novel Chromophoric Substrates†

John D. Doran,‡ Peter J. Tonge,§ John S. Mort,|| and Paul R. Carey*,⊥

Department of Biochemistry, University of Ottawa, Ottawa, Ontario, Canada K1H 8M5, Department of Chemistry, State University of New York at Stony Brook, Stony Brook, New York 11794, Joint Diseases Laboratory, Shriners Hospital for Crippled Children, 1529 Cedar Avenue, Montreal, Quebec, Canada H3G 1A6, and Department of Biochemistry, Case Western Reserve University, 10900 Euclid Avenue, Cleveland, Ohio 44106

Received March 18, 1996; Revised Manuscript Received May 28, 1996⊗

ABSTRACT: In order to investigate structure−reactivity relationships within a series of acyl cysteine proteases [Doran, J. D., & Carey, P. R. (1996) *Biochemistry 35*, 12495−12502], deacylation kinetics have been measured for a number of acyl intermediates involving members of the papain superfamily. Derivatives of the "simple" chromophoric ligand (5-methylthienyl)acrylate (5MTA) and those based on two chromophorically labeled derivatives of peptidyl substrates, viz., 2-[(*N*-acetyl-L-phenylalanyl)amino]-3-(5-methylthienyl)acrylate (Phe5MTA) and 2-[(*N*-acetyl-L-alanyl)amino]-3-(5-methylthienyl)acrylate (Ala5MTA), were used to create acyl enzyme adducts with papain, cathepsin B, and cathepsin L. The chromophoric specific substrates were designed to utilize hydrogen-bonding and hydrophobic interactions which are known to be important in promoting catalysis by papain. For cathepsins B and L, removing one of the hydrogen-bonding donors making up the putative oxyanion hole retards deacylation by 3−25-fold, demonstrating that the oxyanion hole has a modest effect on catalysis for these substrates. With the above substrates and the wild-type and oxyanion hole mutants, the values of the deacylation rate constants stretch over a 214-fold range, from 0.07 to 15×10^{-3} s^{-1}. The pK_a for deacylation of [(5-methylthienyl)-acryloyl]papain is 4.9, close to that reported for similar papain intermediates, while that for Ala5MTA-papain is at 3.5, which in the latter likely represents the effect of the P_1-S_1 and P_2-S_2 interactions on the environment of histidine-159. For the Phe5MTA-papain the extent of deacylation was found to depend on the pH and the starting acyl enzyme concentration. A simple model has been derived which accounts quantitatively for this behavior, using the assumptions that the protonated form of the acyl product reacylates the enzyme and that in the pH range 5.0−7.5 the ionization of active-site groups has no effect on reacylation. The validity of the first assumption was demonstrated by following the deacylation of Phe5MTA-papain in the presence of the potent inhibitor E-64 [1-(L-*trans*-epoxysuccinyl-L-leucylamino)-4-guanidinobutane], whereupon complete deacylation occurred at all pHs with a pK_a identical to that for Ala5MTA-papain, *viz.*, 3.5.

Members of the papain superfamily of cysteine proteases are widely distributed among living organisms and participate in a number of physiological processes in plants, bacteria, and animals (Brocklehurst *et al*., 1987). There is a considerable amount of evidence implicating cysteine proteases in disease states. In particular, lysosomal cathepsins are believed to be involved in several pathological conditions such as muscular dystrophy (Katunuma, 1987), rheumatoid arthritis (Werb *et al*., 1989), and tumor invasiveness (Sloane, 1990). Thus, interest in the detailed mechanisms of cathepsins such as B and L is enhanced by their being potential targets for inhibitor-based drug design. For all enzymes in the papain super family, the overall hydrolytic mechanism can be represented minimally by a three-step process as shown in Scheme 1.

Scheme 1

$$E + S \underset{k_{-1}}{\overset{k_{+1}}{\rightleftharpoons}} ES \xrightarrow{k_{+2}} EA + \text{product 1} \xrightarrow{k_{+3}} E + \text{product 2}$$

The free enzyme and substrate (E + S) associate to form a Michaelis complex (ES) with a dissociation constant K_s ($=k_{-1}/k_{+1}$). The carbonyl carbon of the scissile ester or amide bond undergoes nucleophilic attack from the active-site cysteine (Cys-25 in papain), forming the covalent acyl enzyme intermediate (EA) and releasing the alcohol or amine product (product 1) with an acylation rate constant k_{+2}. The acyl enzyme then deacylates with a rate constant k_{+3} by undergoing nucleophilic attack by a water molecule to yield the free enzyme and the carboxylic acid product (product 2). The acylation and deacylation steps are believed to proceed through tetrahedral intermediates (Brocklehurst *et al*., 1987), where the negative charge on the oxygen atom is stabilized by oxyanion hole interactions comprising the N−H from the backbone peptide linkage of Cys-25 and the side chain of Gln-19 in the case of papain. While the role of oxyanion hole interactions in serine proteases is well-established, its function in cysteine proteases has been controversial (Asboth *et al*., 1985; Mackenzie *et al*., 1986). However, experiments in which papain's Gln-19 has been

† This work was supported by the Natural Sciences and Engineering Research Council of Canada and by NIH Grant GM-54072-01 (to P.R.C.).

* Author to whom correspondence should be addressed.
‡ University of Ottawa.
§ SUNY at Stony Brook.
|| Shriners Hospital for Crippled Children.
⊥ Case Western Reserve University.

⊗ Abstract published in *Advance ACS Abstracts,* September 1, 1996.

S0006-2960(96)00648-4 CCC: $12.00

replaced by other amino acids have shown that the oxyanion hole does indeed play a role in cysteine protease catalysis, although for the latter the stabilization of the transition state may be 0.5−1.0 kcal/mol less than in the case of the stabilization of transition states by the oxyanion holes in serine proteases (Ménard *et al*., 1995)

The overall purpose of this and the accompanying paper (Doran & Carey, 1996) is to establish structure−reactivity relationships for the deacylation step of a series of cysteine proteases, including papain, cathepsin B, and cathepsin L. Oxyanion hole mutants of cathepsins B and L were also used to evaluate the contributions of the oxyanion hole to this process. Structural information is accessed through Raman and electronic absorption spectral data on acyl enzymes of these proteases (Doran & Carey, 1996). Extensive and detailed structure−reactivity relationships have been reported by our laboratory for a series of acyl serine proteases (Tonge & Carey, 1989b, 1990, 1992; Carey & Tonge, 1995) and confirmed by other workers (Whiting & Peticolas, 1994). A linear relationship was established between the length of the acyl C═O bond and the logarithm of the deacylation rate constant, and it was possible to use resonance Raman data to establish the strength of the oxyanion hole-to-C═O hydrogen bonds throughout the series (Tonge & Carey, 1992). There are several marked differences in the properties of serine and cysteine acyl enzymes; in the relative importance of the oxyanion hole (Ménard *et al*., 1995), in the intrinsic chemical differences between esters and thiol esters (Grunwell *et al*., 1977; Smolders & Zeegers-Huyskens, 1988), and in the presence of strong electron polarization forces in cysteine protease active sites which appear to be absent in serine proteases (Carey *et al*., 1978). It is these differences which motivated us to explore structure−reactivity relationships for cysteine protease acyl enzymes in the present work.

Arylacryloyl substrates, such as that based on (5-methylthienyl)acrylate (5MTA),[1] are poor substrates for cysteine proteases, with deacylation rates for the corresponding acyl enzymes that are 1000-fold less than those obtained with specific ester and amide substrates. For papain−inhibitor complexes based on specific substrates, X-ray crystallographic experiments by Drenth *et al*. (1976) identified the importance of hydrogen bonds involving P_1NH···O═C (Asp-158), P_2NH···O═C (Gly-66), and P_2C═O···HN (Gly-66). The energetic contributions for each of these interactions, as well as that for a Phe at the substrates' P_2 position, were estimated in the kinetic studies of Berti *et al*. (1991) to be in the range of 2.5−4.0 kcal/mol. Given the importance of these contacts, we undertook an approach similar to that of Smolarsky (1978, 1979) to generate specific chromophoric substrates involving the 5MTA group. By placing acetyl-PheNH- at the α-carbon of ethyl cinnamate (structure **4** in Chart 1), Smolarsky created a chromophoric compound capable of engaging in the specific active-site interactions discussed above. We synthesized the three substrates shown

Chart 1

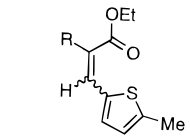

Structure 1

5MTAEt

R:H (1a), NHCOOEt (1b)

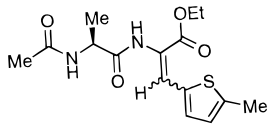

Structure 2

Ala5MTAEt

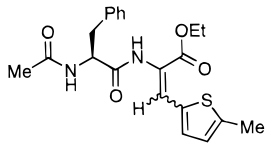

Structure 3

Phe5MTAEt

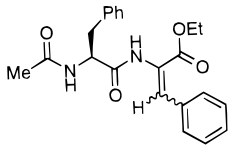

Structure 4

PheCNMEt

in Chart 1 that incorporate 5MTA. Structure **1a** is the nonspecific 5MTA substrate which we have extensively characterized from our previous work on serine proteases (Tonge & Carey, 1990, 1992; Tonge *et al*., 1991, 1993). Structure **1b** explores modulating reactivity which may occur by including a putative hydrogen bond (from NH) at the P_1 position. Structures **2** and **3** are capable of forming favorable hydrogen bonds at both the P_1 and P_2 positions but have different hydrophobic side chains at P_2.

With the above substrates, which have a modest increase in deacylation rate, and oxyanion hole mutants of cathepsin B to retard deacylation, we were able to spread the rates of deacylation over a 200-fold range for a series of acyl cysteine proteases. This represents the range over which we can explore structure−reactivity correlations in the accompanying paper. The present paper presents some details of the kinetic properties of simple and specific (e.g., structure **3**) chromophoric substrates reacting with papain, with cathepsins B and L, and with oxyanion hole mutants of cathepsins B and L. While characterizing the kinetics of the specific substrate, structure **3**, we observed apparent anomalies in the deacylation kinetics. These could be resolved by developing a model where the protonated form of the product (-COOH) acts as an acylating agent.

MATERIALS AND METHODS

Papain, purchased from Sigma, was purified on an agarose mercurial column and then by ion exchange HPLC as described previously (Kim & Carey, 1991). Active-site titrations with PDS demonstrated that the preparations used were 99−100% active. At pH 4.0, PDS reacts rapidly and in stoichiometric amounts with active-site SH groups to produce pyridine-2-thione, $\lambda_{max} = 343$ nm, $\epsilon = 8080$ M^{-1} cm^{-1} (Brocklehurst *et al*., 1987). In conjunction with the extinction coefficient for papain, $\epsilon_{280} = 56\,000$ M^{-1} cm^{-1} (Brocklehurst & Little, 1973), the amount of product released is used to determine the percentage of active enzyme.

[1] Abbreviations: CBZ-Phe-Arg-MCA, carbobenzoxy-L-phenylalanyl-(7-amino-4-methylcoumarinyl)-L-arginine; E-64, 1-(L-*trans*-epoxysuccinyl-L-leucylamino)-4-guanidinobutane; PDS, 2,2′-dipyridyl disulfide; DTT, dithiothreitol; Mes, 2-(*N*-morpholino)ethanesulfonic acid; bicine, *N*,*N*-bis[2-hydroxyethyl]glycine; 5MTAIm, imidazolyl (5-methylthienyl)acrylate; 5MTAEt, ethyl (5-methylthienyl)acrylate; Phe5MTAEt, ethyl 2-[(*N*-acetyl-L-phenylalanyl)amino]-3-(5-methylthienyl)acrylate; Ala5MTAEt, ethyl 2-(*N*-acetyl-L-alanyl)amino]-3-(5-methylthienyl)-acrylate; PheCMNEt, ethyl 2-(*N*-acetyl-L-phenylalanyl)amino]-3-cinnamate.

Imidazolyl (5-methylthienyl)acrylate was synthesized as described previously (Tonge & Carey, 1989a). Syntheses of NHCOOEt5MTA, Phe5MTA, and Ala5MTA ethyl esters were undertaken according to the methods in Doran *et al*. (1995).

Molecular Biology. Ultracompetent XL2-Blue *Escherichia coli* cells were purchased from Stratagene (La Jolla, CA) and restriction enzymes and alkaline phosphatase were from Boehringer Mannheim (Laval, Quebec, Canada). DNA purification was accomplished using either a Prep-A-Gene DNA purification kit from Bio-Rad (Mississauga, Ontario, Canada) or the Magic Minipreps DNA purification system from Promega. Sheep anti-human cathepsin B (Mort *et al*., 1981) and rabbit anti-human procathepsin L (Y. Iwata, E. R. Lee, H. Tateishi, C. P. Leblond, and J. S. Mort, manuscript in preparation) were used for immune detection of expressed proteins on Western blots using the Protein G gold Immun-Blot assay kit from Bio-Rad. Oligonucleotides were synthesized with a Beckman oligo-1000 synthesizer. Polymerase chain reaction (PCR) was performed using a Hybaid Omni Gene PCR machine.

The cDNA for human procathepsin L was amplified by PCR from a reverse-transcribed RNA preparation obtained from human cartilage and ligated, in frame, into the *Hin*dIII site of the yeast α-factor cassette which had been previously inserted into the multiple purpose shuttle vector pVT105, a variant of the pVT100U series (Vernet *et al*., 1987) lacking the alcohol dehydrogenase promoter. A similar construct for the expression of rat cathepsin B was used as described previously (Rowan *et al*. 1992). The mutations Q19S for human cathepsin L and Q23A and Q23S for rat cathepsin B were prepared by site-directed mutagenesis using the method of Kunkel *et al*. (1987). Protein was expressed in *Saccharomyces cerevisiae* strain BJ3501; however, yields from this system were low for the oxyanion hole mutants (0.1−1 mg/L) so the constructs were transferred to the *Pichia pastoris* expression system (Invitrogen, San Diego, CA). This system uses the AOX1 promoter and methanol as an inducer and is reported to provide 10−100-fold higher heterologous protein expression levels than can be obtained using *S. cerevisiae* (Cregg *et al*., 1993).

The prepro-α-factor-procathepsin B and prepro-α-factor-procathepsin L constructs were transferred from the original plasmids to the pHIL-D2 *P. pastoris* vector using a variation of the *in vivo* recombination strategy of Jones and Howard (1992). This strategy places the α-factor construct upstream of the AOX1 promoter leading to secretion of the procathepsins B and L. The desired inserts were amplified by PCR using the appropriate primers so that they could be recombined by *E. coli in vivo* with pHIL-D2 cut at the single *Eco*RI site at position 957. Primers were designed to be complementary to both a section of the pHIL-D2 sequence adjacent to the single *Eco*RI cut site and to the relevant DNA segment of the insert to be amplified. As an example, the following two primers were synthesized for amplification of the prepro-α-factor-procathepsin L construct. For the 3′ primer the oligonucleotide 5′-CAGTCATGTCTAAGGCTCACACAGTGGGGTAGCTGG-3′ was synthesized in which the first 17 nucleotides are complementary to base pairs 961−977 of the sense strand of pHIL-D2 while the remaining nucleotides are complementary to the 3′ end of the antisense strand of the cathepsin L cDNA. For the 5′ primer the oligonucleotide 5′-ACTAATTATTCGAAACGATGAGATTTCCTTCAATTTTTAC-3′ was synthesized in which the first 17 base pairs are complementary to nucleotides 937−953 of the antisense strand of pHIL-D2 while the remaining nucleotides are complementary to the 5′ end of the sense strand of the prepro-α-factor-procathepsin L construct representing the beginning of the α-factor presequence. These primers were used to amplify the prepro-α-factor-procathepsin L construct by PCR using the original plasmid as the template. The resultant fragment was mixed with pHIL-D2 plasmid cut at the *Eco*RI site. The ends originating from the cut site were dephosphorylated using alkaline phosphatase in order to minimize *in vivo* recombination without incorporation of the required insert. The DNA mixture was then used to transform competent *E. coli* following the Stratagene procedure. Colonies were selected for ampicillin resistance and the resultant clones were screened for incorporation for the appropriate insert by agarose gel electrophoresis. On average about 25% of the clones contained the required insert. The validity of all constructs used for *P pastoris* transformation was confirmed by DNA sequencing.

The pHIL-D2 plasmids containing the desired inserts were transformed into *P. pastoris* strain GS115 according to the manual's instructions. Protein expression by yeast transformants was gauged qualitatively by SDS−polyacrylamide gel electrophoresis and Western blots. The transformants giving the best expression were then used for large-scale preparations which typically gave yields of 1−50 mg/L. The large-scale protocol consisted of 2 days growth in 2 L of minimal glycerol medium. The cells were then separated by centrifugation and suspended in 1 L of minimal methanol medium for 3 days of growth.

Protein Purification. After completion of the growth in minimal methanol medium, the cells were harvested by centrifugation and the medium containing the secreted recombinant protein was concentrated to 50 mL using a Millipore Pellicon Cassette concentrator followed by an Amicon stirred cell concentrator (YM-10 membrane). The concentrated medium was then dialyzed in 20 mM citrate buffer, pH 4.7. Acidification of the medium during the dialysis permits both wild-type cathepsins B and L to autoprocess themselves from the proenzyme form to the catalytically active enzyme (Rowan *et al*. 1992). The oxyanion hole mutants were processed to mature enzyme using pepsin as described by Rowan *et al*. (1992).

A two-step column purification procedure was used to purify the enzymes to homogeneity. An initial purification to remove the majority of the medium components was accomplished by binding the enzyme to a CM-Sepharose fast-flow resin equilibrated with 20 mM acetate buffer, pH 5.0. The buffer was run through the column until all traces of the colored medium components were removed. The bound enzyme was then batch-eluted with buffer containing 1 M NaCl. For wild-type and mutant cathepsin B enzymes the eluent was concentrated to 10 mL using an Amicon concentrator. During concentration the buffer was exchanged to 50 mM phosphate and 1 mM EDTA, pH 6.0. The concentrated solution was then purified using an agarose-Asx-Gly-Phe-Gly-semicarbazone resin as described by Fox *et al*. (1992). For cathepsin L and the Q19S mutant the eluent was concentrated as for the cathepsin B enzymes except that the buffer was exchanged with 50 mM formate and 1 mM EDTA, pH 4.0. The concentrated solution was

then applied to a thiolpropyl-Sepharose 6B column equilibrated with the pH 4.0 buffer. The column was washed with 10 volumes of the pH 4.0 buffer and then the bound enzyme was eluted using 50 mM phosphate buffer, pH 6.0, containing 5 mM dithiothreitol (DTT). The eluted enzyme was then exchanged with three times 40 mL of 50 mM formate buffer, pH 4.0, with an Amicon in order to remove excess DTT, and was then concentrated to a final volume of 2 mL. This was then dialyzed overnight against the pH 4.0 buffer containing 1.5 mM 2,2′-dipyridyl disulfide (PDS). The protected enzyme was then stored at 4 °C until needed.

Preparation of Acyl Enzymes. Two hundred microliters of a 0.54 mM solution of papain, pH 4.0, was activated with DTT (final concentration 2 mM) for 15 min. To prepare Phe5MTA-papain, 30 μL of a 35 mM solution of Phe5MTA ethyl ester or Phe5MTA acid in DMSO was added to the activated papain solution and allowed to react for 3 min. The excess substrate was then removed by centrifugation through a 1-mL G-25 column equilibrated with 5 mM formate and 1 mM EDTA, pH 4.0. To prepare 5MTA-papain and Ala5MTA-papain, the more reactive imidazole derivatives had to be employed as acylating agents. In this case activated papain had to be centrifuged through the same aforementioned G-25 column in order to remove excess DTT (which reacts with the imidazole derivatives). The resulting DTT-free activated papain was then reacted with either 30 μL of a 35 mM solution of 5MTA Im or Ala5MTA Im in DMSO. The Ala5MTA Im was found to be unstable and therefore it had to be generated *in situ*. This was done by adding a stoichiometric amount of 1,1-dicarbonylimidazole to Ala5MTA acid just prior to the acylation reaction with enzyme. After 3 min of acylation, the resultant acyl enzyme was purified via G-25 column centrifugation as described previously. 5MTA-papain has a λ_{max} of 378 nm for the bound chromophore, while both Phe5MTA-papain and Ala5MTA-papain have λ_{max} at 384 nm. Similar procedures were used to prepare acyl cathepsin B complexes.

Deacylation Kinetics. Deacylation kinetics were determined using a Cary 3 UV−visible spectrophotometer. Deacylation reactions were initiated by diluting the desired acyl enzyme into 1 mL of buffer. Buffer solutions were (1) pH range 3−3.75 and 5.0−5.5, 50 mM citrate; (2) pH range 4.0−4.5, 50 mM formate; (3) pH 6.0, 50 mM 2-(*N*-morpholino)ethanesulfonic acid (Mes); (4) pH range 6.5−7.5, 50 mM phosphate; (5) pH 8.5, 50 mM *N*,*N*-bis[2-hydroxyethyl]glycine (bicine). All deacylation buffer solutions also contained 0.2 M NaCl (in order to maintain constant ionic strength), and 1 mM EDTA. For some experiments involving Phe5MTA-papain, the buffer solution also contained 1-(L-*trans*-epoxysuccinyl-L-leucylamino)-4-guanidinobutane (E-64) purchased from Boehringer Mannheim. Deacylation kinetics were monitored at 390 nm at 25 °C. Rate constants were evaluated by fitting the data to a first-order exponential equation using the program Enzfitter (Elsevier-Biosoft). The pK_as for deacylation of 5MTA-papain, Ala5MTA-papain, and Phe5MTA-papain in the presence of E-64 were evaluated by fitting the data to

$$y = Cx[10^{(pH-pK_a)}]/[10^{(pH-pK_a)} + 1] \quad (1)$$

where C = upper limit for the rate constant.

Base-catalyzed deacylation in the presence of 1.0 M NaOH was monitored in the same manner. The second-order rate constant for this process ($k_{[OH^-]}$) was obtained by dividing the apparent first-order rate constant by the concentration of OH^-.

Steady-State Kinetics. Steady-state kinetic assays were performed in 50 mM bicine, 0.2 M NaCl, and 1 mM EDTA at pH 8.5 containing 20% (v/v) acetonitrile at 25 °C. Lucas and Williams (1969) have shown that in 20% (v/v) acetonitrile−water there is little change in the kinetic parameters for the papain-catalyzed hydrolysis of *N*-benzoylglycine methyl ester compared to water alone. Initial velocities for hydrolysis of either Phe5MTA or Ala5MTA ethyl ester were determined at a constant papain concentration of 6.8 μM while the substrate concentrations were varied. The reactions were monitored at 350 nm so that the initial rate of disappearance of reactant could be freely monitored without interference from the product absorption band. Michaelis−Menten parameters k_{cat} and K_m were determined from the initial velocities by Hanes−Woolf plots.

Dissociation Constant Evaluation. The following procedure was carried out to evaluate K_d (i.e., K_i) for Phe5MTA-papain at various pH values. The ratio of the 280-nm protein band to the 384-nm bound chromophore band was determined to be 2.5 at pH 4.0 for an 11 μM solution. The acyl enzyme complex is sufficiently stable under these conditions so that this ratio may be used to represent 100% acylation. Concentrated Phe5MTA-papain at pH 4.0 was diluted to a given concentration into a buffer of the desired pH. The variation with time of the 384-nm band was used to verify that the system had attained equilibrium. By using the 280-nm/384-nm ratio of 2.5 and the measured concentration of protein in the sample, it is possible to calculate that the percentage of acyl enzyme remaining is equal to ($100A_{384}/A^0_{384}$), where $A^0_{384} = A_{280}/2.5$, the magnitude of the 384-nm band before deacylation (i.e., representing 100% acylation) and A_{384} is the absorbance at 384 nm at equilibrium.

Once the percentage acyl enzyme has been determined, it is possible to calculate the concentrations of acyl enzyme, free enzyme, and free product due to the 1:1:1 stoichiometry of the reaction. K_i^{app} may then be evaluated using

$$K_i^{app} = [\text{free enzyme}][\text{free product}]/[\text{acyl enzyme}] \quad (2)$$

In order to calculate K_i^{app} corrected for product ionization, the Henderson−Hasselbalch equation was used to calculate the degree of product ionization at the desired pH. A pK_a of 3.8 was determined spectrophotometrically for Phe5MTA acid. The calculated protonated product concentration was then substituted into the K_i^{app} equation for [free product] as shown in eq 3. The corrected value of K_i^{app} is designated K_i.

$$K_i = [\text{free enzyme}][\text{protonated product}]/[\text{acyl enzyme}] \quad (3)$$

RESULTS AND DISCUSSION

Comparison of Deacylation Rate Constants for Acyl Enzymes Derived from Specific and Nonspecific Substrates. Each of the 5MTA substrates can be used to generate a chromophoric acyl enzyme complex, consistent with deacylation being rate-limiting for esters. These acyl enzymes are most stable at pH 4 and will deacylate rapidly and completely when the pH is raised to a value, above pH 6.0, where deacylation is maximal. Since the acyl enzyme complexes

Table 1: Deacylation Rates of Acyl Cysteine Proteases[a]

acyl enzyme	deacylation rate at active pH ($s^{-1} \times 10^{-3}$)
5MTA-papain (5)	1.1
NHCOOEt5MTA-papain	1.0
Phe5MTA-papain (7)	3.3
Ala5MTA-papain	3.3
5MTAcatBwt (3)	0.5
Phe5MTAcatBwt (6)	2.8
5MTAcatBQ23A (2)	0.18
5MTAcatBQ23S (1)	0.07
Phe5MTAcatBQ23S (4)	0.6
5MTAcatLwt (8)	7.7
Phe5MTAcatLwt (10)	15
5MTAcatLQ19S (9)	0.3

[a] The numbering scheme is in accordance with that used for the acyl enzymes in the accompanying paper (Doran & Carey, 1996).

Table 2: Rate Constants for the Hydrolysis of Ethyl Ester Substrates and Their Corresponding Acyl Papains

substrate	$k_{[OH^-]}$[a] ($M^{-1}\ s^{-1} \times 10^{-3}$)	k_{obs} for acyl papain ($s^{-1} \times 10^{-3}$)	ratio $k_{obs}/k_{[OH^-]}$
5MTAEt	23	1.1	0.05
NHCOOEt5MTAEt	2.9	1.0	0.34
Phe5MTAEt	0.50	3.3	6.6
Ala5MTAEt	0.65	3.3	5.1

[a] Hydrolysis rates were determined at pH 14.0, 25 °C.

display a characteristic absorption band near 380 nm, deacylation rates can be measured conveniently by following changes in absorbance as a function of time. The results for a series of such acyl enzymes are reported in Table 1. The 5MTA-papain acyl enzyme deacylates with a rate constant of 0.0011 s^{-1}, and attachment of the NHCOOEt moiety to the α-carbon of 5MTA has no effect on the deacylation rate with papain. There is, however, a 3-fold increase in deacylation with either the Phe5MTA- or Ala5MTA-papain acyl enzymes. The increase in deacylation rate on going from 5MTA- to Phe5MTA-based acyl enzymes is also observed with cathepsins B and L, where k_3 increases by 6-fold and 2-fold, respectively. Even though these increases are modest, they suggest that the presence of P_1-S_1 and P_2-S_2 contacts can contribute to accelerate deacylation.

Table 2 contains the second-order rate constants for base-catalyzed hydrolysis of the ethyl esters **1a**, **1b**, **2**, and **3** and the ratio to the hydrolysis rate of the corresponding acyl papain complex. Contrary to the effect observed on enzyme-catalyzed deacylation, the attachment of a peptide moiety to the α-carbon of 5MTA results in a decrease in the base-catalyzed hydrolysis of the peptide 5MTA esters compared to the nonspecific 5MTA ester. Phe5MTAEt is 46-fold less reactive than 5MTAEt toward base-catalyzed hydrolysis, and yet Phe5MTA-papain deacylates faster than 5MTA-papain by a factor of 3. Assuming that the corresponding thiol ethyl esters show the same trend in base-catalyzed hydrolyis rates as the ethyl esters, the data in Table 2 indicate that papain-catalyzed deacylation is accelerated by approximately 100-fold for the Phe5MTA acyl enzyme compared to the nonspecific 5MTA-papain. Thus, the interactions of the dipeptide moiety with papain's active site contribute significantly to increase the deacylation rate and compensate for the lower susceptibility to hydrolysis inherent within the structures of Ala5MTA and Phe5MTA. The incremental effects on $k_3/k_{[OH^-]}$ observed upon attachment of NHCOOEt and of the either of the dipeptide moieties to 5MTA are reminiscent of those observed by Berti *et al*. (1992) for a variety of substrates that measured the different contributions made by S_1-P_1 and S_2-P_2 hydrogen bond contacts to the catalytic rate. Hence, it can be concluded that the P_1 amide (as evinced by the NHCOOEt5MTA acyl enzyme) and the P_2 amide and the P_2 C═O (evinced by Phe5MTA and Ala5MTA acyl enzymes) are making significant contributions to deacylation rate enhancement. Exchanging Phe for Ala in the dipeptide 5MTA ester has only a small effect on the base-catalyzed hydrolysis rate and none on k_3 for the acyl papain complex.

Table 3: Kinetic Constants for Papain-Catalyzed Hydrolysis Determined by Steady-State Kinetics

substrate	k_{cat} ($s^{-1} \times 10^{-3}$)	K_m ($M \times 10^{-3}$)	k_{cat}/K_m ($s^{-1}\ M^{-1}$)
5MTA ethyl ester			<0.07
NHCOOEt5MTA ethyl ester			<0.07
Ala5MTA ethyl ester	3.3	3.9	0.85
Phe5MTA ethyl ester	3.3	0.062	53

For comparison, the parameters k_{cat} and K_M for hydrolysis of the ethyl ester substrates have been determined using steady-state kinetics and are shown in Table 3. As mentioned previously, deacylation is rate-limiting for the substrates used in this study and, accordingly, k_{cat} was found to be equal to k_3, the rate constant of deacylation obtained through deacylation kinetic measurements. It can be seen that the presence of the dipeptide moieties in Ala5MTAEt and Phe5MTAEt results in a major increase in k_{cat}/K_M compared to the nonspecific 5MTAEt and NHCOOEt5MTAEt substrates. The steady-state kinetic parameters for the latter two substrates could not be obtained since the reaction was too slow even at concentrations of 3 mM, which approaches their solubility limits in the assay buffer, and only an upper limit to k_{cat}/K_M is presented in Table 2. The Phe5MTAEt is a better substrate than Ala5MTAEt, the value of k_{cat}/K_M being 62-fold higher with Phe5MTAEt than with Ala5MTAEt. This illustrates the significant contribution of S_2-P_2 interactions to enzyme-catalyzed hydrolysis of this type of substrates and reflects the well-known specificity of papain for hydrophobic side chains in the P_2 position of substrates (Brubacher & Zaher, 1979; Lowe & Yuthavong, 1971). This preference for Phe over Ala in P_2 is not observed for deacylation rates.

Extending the Range of Deacylation Rate Constants by the Use of Oxyanion Hole Mutants. To provide a better basis for the establishment of structure−activity relationships using Raman and absorption spectroscopies, it is important to have acyl enzyme complexes with as wide a range of deacylation rate constants as possible. For this purpose, we have also measured the deacylation rate constants for oxyanion hole mutants of the cysteine proteases cathepsin B and L. The effect of these mutations on the rate of deacylation is reported in Table 1. Replacing Gln23 by Ala or Ser in cathepsin B results in a 3−7-fold decrease in deacylation rate while the mutation of Gln19 to Ser in cathepsin L causes a 26-fold decrease. These mutations have been shown to decrease k_{cat}/K_M for hydrolysis of *Z*-Phe-Arg-MCA by approximately 60−600-fold in papain (Ménard *et al*., 1991) and 12−100-fold in cathepsin B (unpublished data). The influence of oxyanion hole mutations on deacylation reported in the present study confirms that oxyanion hole interactions are also operational

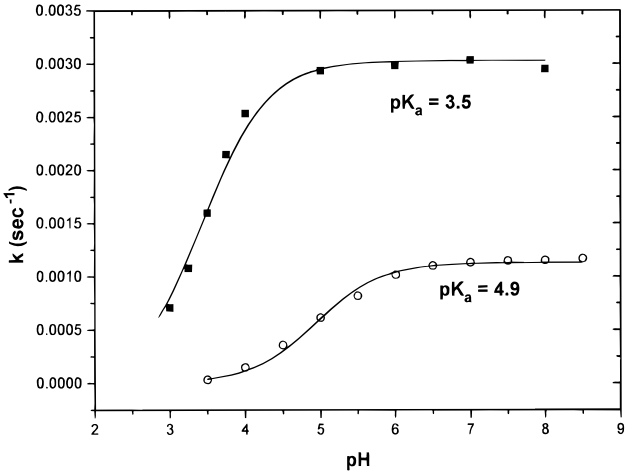

FIGURE 1: Plots of deacylation rate constant vs pH for 5MTA-papain (○) and Ala5MTA-papain (■). The pK_as were evaluated as described under Materials and Methods.

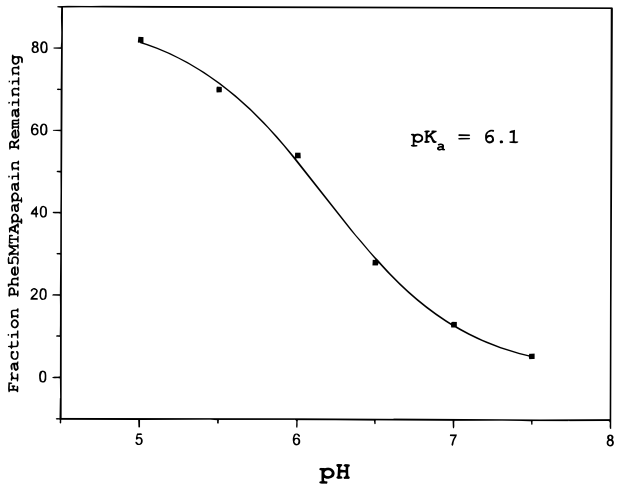

FIGURE 2: Plot of the fraction of Phe5MTA-papain remaining at equilibrium vs pH.

in the deacylation process, but possibly to a lesser extent than in acylation. More importantly, the use of these mutants has allowed us to expand the range of deacylation rates from 15×10^{-3} s^{-1} with Phe5MTA-catL down to 0.07×10^{-3} s^{-1} with 5MTA-catBGln23Ser.

pH Dependency of Deacylation. The influence of pH on deacylation rates was determined for 5MTA-, Ala5MTA- and Phe5MTA-papain. Results for the first two acyl enzymes are shown in Figure 1. The nonspecific 5MTA-papain has a deacylation pK_a of 4.9, which is similar to the pK_a value obtained for cinnamoyl-papain, which has a deacylation pK_a of 4.7 (Bender & Brubacher, 1964). The deacylation pK_a of Ala5MTA-papain, however, is 3.5, more than 1 pH unit lower than that for 5MTA-papain. Assuming that this pK_a represents ionization of the active-site His159 residue, one interpretation of this result is that the presence of the dipeptide moiety containing S_1-P_1 and S_2-P_2 contacts lowers the pK_a of His159 in the acyl enzyme by lowering the effective dielectric constant near the side chain.

For the Phe5MTA-papain, complex deacylation profiles were obtained. At low pH little or no deacylation occurs. As the pH is raised, successively larger proportions of the total acyl enzyme deacylates. This is illustrated in Figure 2, where the acyl enzyme population was 11 μM at pH 4.0 and the mole fraction of Phe5MTA-papain at equilibrium is

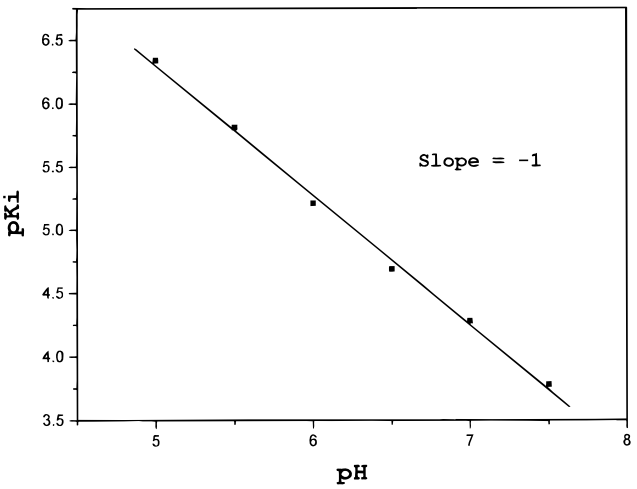

FIGURE 3: Plot of pK_i^{app} vs pH for Phe5MTA-papain. The pK_i^{app} was evaluated using eq 2, as described under Materials and Methods.

Table 4: Values of pK_i' Determined by Assuming Only the Protonated Form of the Product Binds to Papain[a]

pH	pK_i'
5	7.6
5.5	7.2
6.0	7.4
6.5	7.4
7.0	7.5
7.5	7.4

[a] The average value of pK_i' is 7.42.

plotted as a function of pH. Under these conditions half the population of the acyl enzyme is seen to deacylate at pH 6.1. A very similar effect was observed by Smolarsky when he studied the extent of acyl papain formation by the acid product PheCNM acid as a function of pH (Smolarsky, 1978). He ascribed the pH dependence as due to ionization of one or more of papain's active-site residues. Other workers have also observed strong inhibition of papain activity by acid product molecules (Sluyterman, 1964; Berger & Schecter 1970), where the latter authors considered the possibility that the pH dependence of inhibition could be explained, at least in part, by only the protonated form of the product (-COOH) being in equilibrium with the enzyme. If we, too, make the assumption that only the protonated form of the product, Phe5MTACOOH, reacylates papain, we can reproduce quantitatively the complex deacylation profiles.

A plot of pK_i^{app} values calculated using eq 1 from Materials and Methods, against pH is shown in Figure 3. In eq 1 the *total* product concentration is used to calculate each pK_i^{app}. The slope of -1 in Figure 3 shows that a single negative charge is being generated in that pH range when the complex dissociates into free enzyme and ligand (Dixon & Webb, 1979). For Phe5MTA-papain, the product is negatively charged in the pH range 5.0−7.5, and this suggests that it gives rise to the observed slope of -1. However, when only the protonated form of the product is used to calculate pK_i in eq 2, the pK_i is pH-independent as seen in Table 4. This finding suggests strongly that, in the pH range 5.0−7.5, the increasing K_i^{app} values in Figure 3 are due to the protonation state of the product (inhibitor). In the Appendix, we have expanded on the ideas inherent in eqs 1 and 2 to produce a

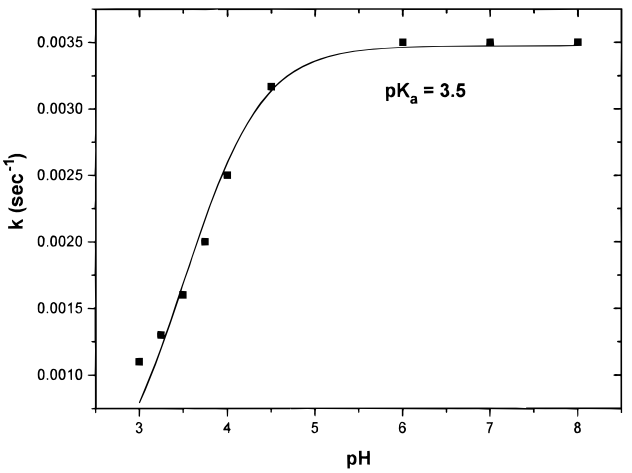

FIGURE 4: Plot of the deacylation rate constant vs pH for Phe5MTA-papain. Deacylation kinetics were measured in the presence of 118 μM E-64.

simple mathematical model which predicts the deacylation behavior of systems such as Phe5MTA-papain. The model makes two assumptions, that only the protonated form of the product (-COOH) rebinds to the active site and that, in the pH range of concern, binding is unaffected by possible ionizations of active-site amino acid side chains.

The first assumption was tested in part by following the deacylation of Phe5MTA-papain in the presence of the powerful cysteine protease inhibitor E-64. The rationale behind this experiment was that E-64 would completely prevent reacylation by Phe5MTACOOH. That this is indeed the case is shown by the data in Figure 4. Complete deacylation was obtained at all pHs with a pK_a of 3.5. This pK_a is identical to that of the Ala5MTA-papain, and the deacylation rate constants of the two acyl papains are very similar at any given pH. This is consistent with the conclusions drawn from the data in Table 2 that the effects of the Phe side chain operate in the acylation process. Other workers have reached similar conclusions. Lowe and Yuthavong (1971) determined that the papain-catalyzed deacylation rates for a variety of *N*-acylglycines are relatively constant, while the k_{cat}/K_m values range over factors of 10^5–10^7, with substrates with Phe in the P_2 position giving the highest values. Brubacher and Zaher (1979) found the same behavior for a series of methyl esters, and they concluded that the S_2 site preference for phenylalanine is apparent only in terms of overall reactivity.

The model's second assumption, regarding the insensitivity of binding to active-site ionizations, was tested by predicting the effects of initial acyl enzyme concentration on the final equilibrium concentration at any given pH. Figure 5 contains simulations, using the equations in the Appendix, illustrating the effect of changing the initial acyl enzyme concentration on the final equilibrium concentration of Phe5MTA-papain. The apparent p*K* shifts to lower values as the acyl enzyme concentration decreases—as the initial concentration of acyl enzyme becomes lower, the reacylation process becomes less significant. This process was verified experimentally. When an 11 μM solution of Phe5MTA-papain, stable at pH 4.0, was diluted 10-fold in the same pH 4.0 buffer, the acyl enzyme proceeded to deacylate. Thus, the p*K* of 6.1 derived from Figure 2 indicating half of the acyl enzyme deacylation is only valid for an 11 μM solution of Phe5MTApapain. Equation A9 (Appendix) may be used to predict the p*K* that

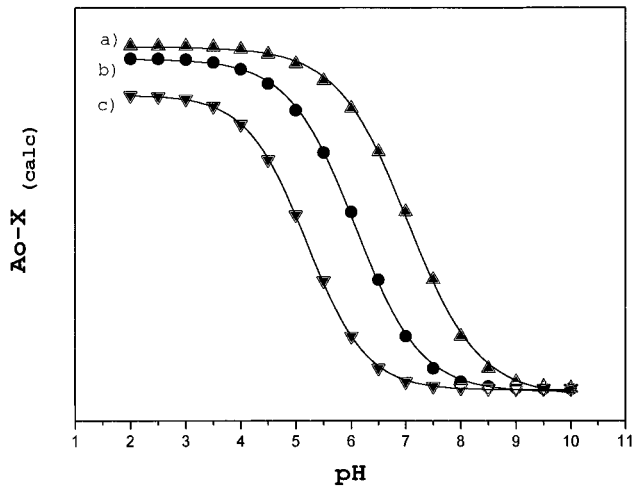

FIGURE 5: Simulation curves illustrating the effect the initial acyl enzyme concentration, A_0, has on the final equilibrium concentration of Phe5MTA-papain. (a) A_0 = 110 μM, pK_a = 7.0; (b) A_0 = 11 μM, pK_a = 6.1; (c) A_0 = 1.1 μM, pK_a = 5.2. The equations of the Appendix were used to generate the curves. The following values were used for all of the simulations: K_a = 0.00016 M and K = 3.8 $\times$ 10^{-8} M. For the sake of clarity, curves b and c were multiplied by factors of 10 and 100, respectively, so that they appear on the same scale.

will result from an initial starting Phe5MTA-papain concentration of 11 μM and this simulation is shown in Figure 5, curve b. Both the simulation (Figure 5, curve b) and the experimentally determined curve (Figure 2) give a p*K* of 6.1, thus eq A9 from the model predicts correctly the effects of pH on the degree of inhibitor binding to papain. The identity of the experimentally derived p*K* and that derived from the model demonstrates that the assumption that active-site ionizations do not affect binding is valid in the pH range of 5.0–7.5 plotted in Figure 2. In general, compliance with the model can be used to distinguish the effect of ligand or protein ionization on the pH dependence of binding.

ACKNOWLEDGMENT

We are grateful to Drs. R. Ménard and V. E. Anderson for discussions and suggestions.

APPENDIX

Model for pH Dependence of Papain Deacylation–Reacylation. Deacylation is represented as

$$\underset{\text{acyl enzyme}}{[A]} \underset{k'}{\overset{k}{=}} \underset{\text{enzyme}}{[E]} + \underset{\text{product}}{[P]} \qquad \text{(A1)}$$

At equilibrium,

$$[E][P]/[A] = K$$

If A_0 = starting concentration of acyl enzyme, $[A_0 - E] = A$. The total amount of product, P_T, is the sum of the protonated, P_H, and unprotonated, P_U, forms:

$$P_T = P_U + P_H \qquad \text{(A2)}$$

$$P_H \overset{K_a}{=} P_U + [H^+] \qquad \text{(A3)}$$

and

$$[P_U] = K_a[P_H]/[H^+] \qquad \text{(A4)}$$

Substituting $[P_U]$ into eq A2

$$[P_T] = K_a[P_H]/[H^+] + [P_H] \quad \text{(A5)}$$

thus

$$[P_H] = [P_T]/(1 + K_a/[H^+]) \quad \text{(A6)}$$

If we assume that only the protonated product, P_H, participates in the equilibrium and replace P in eq A1 by P_H:

$$K[A_0 - E] = [E]\{[P_T]/(1 + K_a/[H^+])\} \quad \text{(A7)}$$

$[E] = [P_T]$ and thus upon expanding eq A7

$$[P_T]^2 + K(1 + K_a/[H^+])[P_T] - K[A_0](1 + K_a/[H^+]) = 0 \quad \text{(A8)}$$

Solving for P_T:

$$2P_T = -K(1 + K_a/[H^+]) \pm \{(K(1 + K_a/[H^+]))^2 + 4K[A_0](1 + K_a/[H^+])\}^{1/2} \quad \text{(A9)}$$

Using eq A9 we can determine the equilibrium concentration of any species provided that the equilibrium constant K (which is equal to K_i, the "true" equilibrium constant involving acyl enzyme, enzyme, and protonated product), initial starting concentration, and K_a of the acid product are known. For Phe5MTA-papain, K is equal to 3.8×10^{-8} M (i.e., the inverse negative logarithm of 7.42, Table 4).

REFERENCES

Asboth, B., Stokum, E., Khan, I. U., & Polgar, L. (1985) *Biochemistry 24*, 606−609.

Bender, M. L., & Brubacher, L. J. (1964) *J. Am. Chem. Soc. 86*, 5333−53334.

Berger, A., & Schechter, I. (1970) *Philos. Trans. R. Soc. London, B 257*, 249−264.

Berti, P. J., Faerman, C. H., & Storer, A. C. (1991) *Biochemistry 30*, 1394−1402.

Brocklehurst, K., & Little, G. (1973) *Biochem. J., 133*, 67−80.

Brocklehurst, K., Willenbrock, F., & Salih, E. (1987) *Hydrolytic Enzymes* (Neuberger, A., & Brocklehurst, K., Eds.) Chapter 2, Elsevier, Amsterdam.

Brubacher, L. J., & Zaher, M. R. (1979) *Can. J. Biochem. 57*, 1064−1072.

Carey, P. R., & Tonge, P. J. (1995) *Acc. Chem. Res. 28*, 8−13.

Carey, P. R., Carriere, R. G., Phelps, D. J., & Schneider, H. (1978), *Biochemistry 17*, 1081−1087.

Cregg, J. M., Vedvick, T. S., & Raschke, W. C. (1993) *Biotechnology 11*, 905−910.

Dixon, M., & Webb, E. C. (1979) Enzymes, 3rd ed., pp 154−157, Longman Group Limited, London.

Doran, J. D., & Carey, P. R. (1996) *Biochemistry 35*, 12495−12502.

Doran, J. D., Tonge, P. J., Carey, P. R., & Arya, P. (1995) *Bioorg. Med. Chem. Lett. 5*, 2381−2384.

Drenth, J., Kalk, K. H., & Swen, H. M. (1976) *Biochemistry 15*, 3731−3738.

Fox, T., De Miguel, E., Mort, J. S., & Storer, A. C. (1992) *Biochemistry 31*, 12571−12576.

Grunwell, J. R., Forest, D. L., Kaplan, F., & Siddigui, J. (1977) *Tetrahedron 33*, 2781−2784.

Jones, D. H., & Howard, B. H. (1992) *Biotechniques 12*, 528−553.

Katunuma, N., & Kominami, E. (1987) *Rev. Physiol. Biochem. Pharmacol. 108*, 1−20.

Kim, M., & Carey, P. R. (1991) *J. Mol. Struct. 242*, 421−431.

Kunkel, T. A., Roberts, J. D., & Zakour, R. A. (1987) *Methods Enzymol. 154*, 367−382.

Lowe, G., & Yuthavong, Y. (1971) *Biochem. J. 124*, 107−115.

Lucas, E. C., & Williams, A. (1969) *Biochemistry 8*, 5125−5135.

Mackenzie, N. E., Grant, S. K., Scott, A. I., & Malthouse, J. P. G. (1986) *Biochemistry 25*, 2293−2298.

Ménard, R., Carriere, J., Laflamme, P., Plouffe, C., Khouri, H. E., Vernet, T., Tessier, D. C., Thomas, D. Y., & Storer, A. C. (1991) *Biochemistry 30*, 8924−8928.

Ménard, R., Plouffe, C., Laflamme, P., Vernet, T., Tessier, D. C., Thomas, D. Y., & Storer, A. C. (1995) *Biochemistry 34*, 464−471.

Mort, J. S., Poole, A. R., & Decker, R. S. (1981) *J. Histochem. Cytochem. 29*, 649−657.

Rowan, A. D., Mason, P., Mach, L., & Mort, J. S. (1992) *J. Biol. Chem. 267*, 15993−15999.

Sloane, B. F., Moin, K., Krepela, E., & Rhozhin, J. (1990) *Cancer Metastasis Rev. 9*, 333−352.

Sluyterman, L. A. A. (1964) *Biochim. Biophys. Acta 85*, 316−321.

Smolarsky, M. (1978) *Biochemistry 17*, 4606−4615.

Smolarsky, M. (1979) *Biochemistry 19*, 478−484.

Smolders, A., Maes, G., & Zeegers-Huyskens, T. (1988) *J. Mol. Struct. 172*, 23−40.

Tonge, P. J., & Carey, P. R. (1989a) *J. Mol. Liq. 42*, 195−212.

Tonge, P. J., & Carey, P. R. (1989b) *Biochemistry 28*, 6701−6709.

Tonge, P. J., & Carey, P. R. (1990) *Biochemistry 29*, 10723−10727.

Tonge, P. J., & Carey, P. R. (1992) *Biochemistry 31*, 9122−9125.

Tonge, P. J., Pusztai, M., White, A. J., Wharton, C. W., & Carey, P. R. (1991) *Biochemistry 30*, 4790−4795.

Tonge, P. J., Carey, P. R., Callender, R., Deng, H., Ekiel, I., & Muhandiram, D. R. (1993) *J. Am. Chem. Soc. 115*, 8757−8762.

Vernet, T., Dignard, D., & Thomas, D. Y. (1987) *Gene 52*, 225−233.

Werb, Z. (1989) Proteinases and matrix degradation, in *Textbook of Rheumatology* (Keller, W. N., Harris, E. D., Ruddy, S., & Sledge, C. S., Eds.) pp 300−321, W. B. Saunders Co., Philadelphia, PA.

Whiting, A. K., & Peticolas, W. L. (1994) *Biochemistry 33*, 552−561.

BI960648H